

Published in final edited form as:

Cancer Res. 2014 February 15; 74(4): 1091–1104. doi:10.1158/0008-5472.CAN-13-1259.

## Activation of the *NOTCH* pathway in Head and Neck Cancer

Wenyue Sun<sup>1</sup>, Daria A. Gaykalova<sup>1</sup>, Michael F. Ochs<sup>2</sup>, Elizabeth Mambo<sup>3</sup>, Demetri Arnaoutakis<sup>1</sup>, Yan Liu<sup>4</sup>, Myriam Loyo<sup>1</sup>, Nishant Agrawal<sup>1</sup>, Jason Howard<sup>5</sup>, Ryan Li<sup>1</sup>, Sun Ahn<sup>1</sup>, Elana Fertig<sup>2</sup>, David Sidransky<sup>1</sup>, Jeffery Houghton<sup>3</sup>, Kalyan Buddavarapu<sup>3</sup>, Tiffany Sanford<sup>3</sup>, Ashish Choudhary<sup>3</sup>, Will Darden<sup>3</sup>, Alex Adai<sup>3</sup>, Gary Latham<sup>3</sup>, Justin Bishop<sup>3</sup>, Rajni Sharma<sup>6</sup>, William H. Westra<sup>1</sup>, Patrick Hennessey<sup>1</sup>, Christine H. Chung<sup>5</sup>, and Joseph A. Califano<sup>1,7,\*</sup>

<sup>1</sup>Department of Otolaryngology-Head and Neck Surgery, Johns Hopkins Medical Institutions, Baltimore, Maryland <sup>2</sup>Department of Oncology and Health Science Informatics, Johns Hopkins Medical Institutions, Baltimore, Maryland <sup>3</sup>Asuragen Inc., Austin, Texas <sup>4</sup>Department of Surgery, Johns Hopkins Medical Institutions, Baltimore, Maryland <sup>5</sup>Department of Oncology, Johns Hopkins Medical Institutions, Baltimore, Maryland <sup>6</sup>Department of Pathology, Johns Hopkins Medical Institutions, Baltimore, Maryland <sup>7</sup>Milton J. Dance Head and Neck Center, Greater Baltimore Medical Center, Baltimore, Maryland

### Abstract

*NOTCH1* mutations have been reported to occur in 10 to 15% of head and neck squamous cell carcinomas (HNSCC). To determine the significance of these mutations, we embarked upon a comprehensive study of *NOTCH* signaling in a cohort of 44 HNSCC tumors and 25 normal mucosal samples through a set of expression, copy number, methylation and mutation analyses. Copy number increases were identified in *NOTCH* pathway genes including the *NOTCH* ligand *JAG1*. Gene set analysis defined a differential expression of the *NOTCH* signaling pathway in HNSCC relative to normal tissues. Analysis of individual pathway-related genes revealed overexpression of ligands *JAG1* and *JAG2* and receptor *NOTCH3*. In 32% of the HNSCC examined, activation of the downstream *NOTCH* effectors *HES1/HEY1* was documented. Notably, exomic sequencing identified 5 novel inactivating *NOTCH1* mutations in 4/37 of the tumors analyzed, with none of these tumors exhibiting *HES1/HEY1* overexpression. Our results revealed a bimodal pattern of *NOTCH* pathway alterations in HNSCC, with a smaller subset exhibiting inactivating *NOTCH1* receptors mutations but a larger subset exhibiting other *NOTCH1* pathway alterations, including increases in expression or gene copy number of the receptor or ligands as well as downstream pathway activation. Our results imply that therapies that target the *NOTCH* pathway may be more widely suitable for HNSCC treatment than appreciated currently.

### Introduction

Head and neck squamous cell carcinoma (HNSCC) is a disease with significant morbidity and mortality. More than 50,000 new cases of HNSCC are diagnosed in the United States yearly, with a mortality rate of 12,000 annually. As with lung cancer, this malignancy is also predominantly related to smoking with alcohol as a co-carcinogen, although infection with the human papillomavirus has also been associated with the majority of oropharynx cancers (1). Despite significant progress in therapeutic interventions, including surgery,

\*Corresponding Author: Joseph A. Califano, MD, Department of Otolaryngology-Head and Neck Surgery, Johns Hopkins Medical Institutions, 1550 Orleans street, Rm 5N. 04, Baltimore, MD 21231. Phone: 410-502-2692; Fax: 410-614-1311; jcalifa@jhmi.edu.

The authors disclose no potential conflicts of interest.

radiotherapy, and chemotherapy, there have been only modest improvements in survival of patients with HNSCC in the past 30 years.

HNSCC, like other solid tumors, develops through a prolonged multistage process involving the accumulation of genetic and epigenetic alterations. Investigators have uncovered several critical genes and pathways important in the tumorigenesis of HNSCC. These include *TP53* (2), *CDKN2A*(3), *Cyclin D1* (4), *PIK3CA* (5), *HRAS*, and *EGFR* (6). However, these molecular alterations do not fully recapitulate the pathogenesis of HNSCC. To gain a comprehensive view of the genetic alteration in HNSCC, Agrawal et al. (7) and Stransky et al. (8) used a high-throughput next-generation sequencing technique to analyze the HNSCC genome. Both groups sequenced the exons of all known human genes in tumor DNA and compared the sequence to that of the corresponding normal DNA from the identical patient. In total, the genomic landscapes of 32 and 74 tumors were examined. Mutations were confirmed in genes that had been previously known to play a role in HNSCC, such as *TP53*, *CDKN2A*, *PIK3CA*, *PTEN*, and *HRAS*. Both research groups reported novel mutations in *NOTCH1*. In both studies, inactivating mutations of *NOTCH1* were found in 10 to 15% of the HNSCC tumors, making *NOTCH1* the second most frequently mutated gene after *TP53*. In several tumors, both alleles harbored mutations in *NOTCH1*. More recently, Pickering et al. have discovered changes in gene copy number and expression for some other *NOTCH* pathway genes including increased copy number changes in *NOTCH* receptor ligands *JAG1* and *JAG2* and in *NUMB* that were associated with elevated mRNA (9).

*NOTCH* signaling pathway has been linked to multiple biological functions, including regulation of self-renewal capacity, cell cycle exit, and survival. The pathway is initiated when one cell expressing the appropriate ligand (Jagged or Delta) interacts with another cell expressing a *NOTCH* receptor (*NOTCH1-4*). Upon ligand binding, the transmembrane *NOTCH* receptor is subsequently cleaved by ADAM metalloprotease and  $\gamma$ -secretase complex. The cleaved product, intracellular fragment of *NOTCH* (NICD), translocates into the nucleus where it interacts with the nuclear DNA-binding factors, CSL/CBF1/RBPjk), and recruits co-activators (MAML proteins) to turn on transcription factors of target genes. The most prominent targets of the *NOTCH* pathway include a set of basic-helix-loop factors of the Hes and Hey families (10, 11). Several studies suggest that *NOTCH* mutation can have either an oncogenic or a tumor-suppressive effect. In T cell acute lymphoblastic leukemia/lymphoma, *NOTCH* signaling had previously implicated as pro-tumorigenic by activating mutations and translocations observed in the genes for *NOTCH* receptors or their regulators (12, 13); whereas in chronic myelomonocytic leukemia, cutaneous, lung and HNSCC tumors, several of the *NOTCH* family mutations in HNSCC encode inactivating mutations, suggesting a tumor suppressor function (14–16).

Due to the discovery of *NOTCH* mutations in HNSCC, a high priority is placed on a more comprehensive understanding of the complex molecular alterations of *NOTCH* signaling pathway in HNSCC. In this study we examined the comprehensive genetic, epigenetic and transcriptional alterations of the *NOTCH* signaling pathway in a cohort of primary HNSCC, and report a systematic dysregulation of the *NOTCH* signaling pathway in HNSCC. Further analysis revealed that the *NOTCH* signaling pathway was activated in a subset of HNSCC tumors, and this pathway activation was independent of the *NOTCH1* mutation status. These findings provide important new insights of *NOTCH* signaling pathway into the pathogenesis of HNSCC and highlight the *NOTCH* pathway as a target for therapeutic development.

## Methods

A more detailed description of our methods and statistical procedures is available in Supplemental Methods.

## Human tissue samples

The tumor tissue samples from patients with HNSCC and normal samples were obtained from patients surgically treated in the Department of Otolaryngology-Head and Neck Surgery at Johns Hopkins Medical Institutions, Baltimore, using appropriate informed consent obtained after institutional review board approval. Microdissection of frozen tumor tissue was done to assure that >80% of tissue contained HNSCC. The normal tissues consisted of tissues obtained from non-cancer affected control patients that underwent uvulopalatopharyngoplasty (UPPP). After review by a pathologist, a section of dissected mucosal layer from discarded UPPP specimens was immediately frozen in liquid nitrogen. All specimens were stored at  $-80^{\circ}\text{C}$  until processing. For microarray analysis, a cohort including 44 HNSCC tumors and 25 normal mucosa tissues was used (Supplementary Table I). For quantitative real-time PCR analysis, in addition to the above cohort used for microarray analysis, two separate cohorts with one comprising of 31 HNSCC tumor tissues and 17 normal mucosa tissues and the other 63 HNSCC tumor tissues and 30 normal mucosa were also used. The application of different cohorts was based on the sample cohort availability.

## DNA extraction and RNA isolation

DNA was extracted from all samples by digestion with  $50\ \mu\text{g}/\text{mL}$  proteinase K (Boehringer, Mannheim, Germany) in the presence of 1% SDS at  $48^{\circ}\text{C}$  overnight, followed by phenol/chloroform extraction and ethanol precipitation (17). Total RNA was isolated with trizol reagent according to the manufacturer's instructions, and then purified with an RNeasy Kit (Qiagen, Germantown, MD).

## HPV analysis

The HPV status was determined as described previously (18). In brief, specific primers and probes have been designed to amplify the E6, E7 regions of HPV16. Their sequences are available in a previous publication. All the samples were run by quantitative Taqman PCR in duplicate. Primers and probes to a housekeeping gene ( $\beta$ -actin) were run in duplicate and parallel to normalize input DNA. HPV copy number more than 1 copy per cell for tumor samples were regarded as positive.

## Copy Number Analysis

The cohort of 44 HNSCC tumor tissues and 25 normal mucosa samples were run on Affymetrix SNP6.0 arrays for copy number analysis. All arrays were run according to the manufacturers' instructions. DNA processing, preparation, hybridization and chip scanning were performed by the Johns Hopkins Microarray Core Facility. The data was normalized using the crlmm package and genome build HG18 annotations (19). The 25 normal mucosa samples and 44 HNSCC samples were then analyzed using the Tibshirani and Hastie outlier statistical approach (20) and compared to 1.74 million values generated by permutation of sample labels to generate an empirical p-value using the approximation of Smyth and Phipson (21). Outlier samples were defined in the standard way.

## Methylation Array Analysis

Bisulfite conversion of genomic DNA from the above cohort was done with the EZ DNA methylation Kit (Zymo Research, D5002) by following manufacturer's protocol with modifications for Illumina Infinium Methylation Assay in the Johns Hopkins microarray core. We have applied the same statistical analysis used for copy number looking for hypomethylation outliers in *NOTCH* pathway genes defined in the Kyoto Encyclopedia of Genes and Genomes (22). *NOTCH* genes with a P value  $<0.05$  were considered significant.

## Gene expression profiling

RNA isolated from the cohort of 44 HNSCC tumor tissues and 25 normal mucosa samples were run on Affymetrix HuEx 1.0 GeneChips for expression analysis. All arrays were run according to the manufacturers' instructions (23–25). To look at the expression of *NOTCH* pathway genes on a tumor sample basis, we compared the expression level of each gene in each individual tumor to the distribution of expression levels in normal mucosa samples assuming a normal distribution. We declared a gene as significantly differentially expressed if the tumor expression level was  $2\sigma$  away from the mean normal expression level, effectively setting a threshold of  $\alpha = 0.05$ .

## Heat map

Heat maps of differential gene expression were created using the R-package gplots. The visualized data comprised gene by sample expression levels, and expression was normalized to Z-score on a gene-by-gene basis to convert all genes to the same scale.

## Gene set analysis

Gene Set Analysis was performed using a mean rank gene set enrichment test (26), as provided in the limma R package (27). Initial gene ranks were generated using an Empirical Bayes statistic. Significance of the *NOTCH* signaling pathway gene set (KEGG database) or Nguyen\_Target\_Set (Molecular Signature Database from the Broad Institute) (28) were measured. Recently, Nguyen identified 85 differentially expressed genes as a gene set (Named as Nguyen\_ *NOTCH1* \_Targets in Molecular Signatures Database of the Broad Institute) of *NOTCH* downstream targets that are concomitantly modulated by activated *NOTCH1* in mouse and human primary keratinocytes (28). With this gene set, we also assessed the expression status of *NOTCH* signaling pathway in the above cohort of HNSCC tumors.

## Exome sequencing of *NOTCH1*

The exome sequencing of *NOTCH1* was performed by Asuragen (Austin, Texas) (29–31). We retained only the high coverage regions for analysis, high coverage being defined by having greater than 10% of the sample median coverage and above 100 reads. We also flagged the loci that are known to have frequent false positive calls in our library. For each set of matched samples, we filtered out variants that were present in the lymphocytes as putative germline variants, or as sample specific systematic error. In our analysis, if the matched normal loci is found to have greater than 1% variant reads, or the variant score difference is within the 99.5% percentile of all pairwise differences for non-annotated loci across the matched pair, the background is considered high and the variant is removed from the list. Variants were annotated using gene structure from the NCBI RefSeq transcript set. Coding base substitutions were classified as missense, nonsense, splice site, or silent. In addition to *NOTCH1*, we also performed targeted sequencing on 51 genes selected from the COSMIC mutation database; those data will be reported separately.

## Quantitative real-time RT-PCR

The same RNA samples used for microarray analysis, the RNA samples from an independent HNSCC cohort as described above, as well as RNA extracted from cell lines were assessed for *NOTCH1*, *HES1* and *HEY1* expression levels using quantitative real-time RT-PCR (Taqman). Reverse transcription was performed with random hexamer primers and Superscript II reverse transcriptase (Invitrogen Corp.) as described previously (17). Quantitative RT-PCR was then carried out on the Applied Biosystems 7900 Sequence Detection Instrument (Applied Biosystems, Carlsbad, CA). The primers and probes (Integrated DNA technologies, San Diego, CA, USA) used in the analysis are available upon

request. In our analysis, serial dilutions of cDNA product for each gene of interest were used for constructing the calibration curves on each plate.

### Immunohistochemistry

56 HNSCC and 11 non-cancer formalin-fixed and paraffin-embedded samples were obtained from the Head and Neck Tissue Bank at Johns Hopkins and were used to construct a tissue microarray under JHU-IRB approved protocols. The protocol incorporated heat-induced antigen retrieval with citrate buffer (pH 6.0) followed by peroxide-blocking step and primary antibody incubation for 15 minutes with rabbit polyclonal antibody against HES1 (Millipore, AB5702, dilution 1: 200), for 30 minutes with rabbit polyclonal antibody against HEY1 (Abcam, ab22614, dilution 1: 200) or 30 minutes with goat polyclonal antibody against cleaved/activated NOTCH1 (Santa Cruz Biotechnology, sc-6014, dilution 1: 400). The tissues were analyzed using Aperio software. The staining was categorized as strong, moderate or none/weak for each individual tissue and averaged for tissue quadruplicates.

### Cell Culture

Human HNSCC cell lines UPCI-SCC090 (090) and SCC61 were used in experiments. 090 was received from Dr. Susanne Gollin, University of Pittsburgh. SCC61 was received from Dr. Ralph Weichselbaum (University of Chicago). In our study, each cell line was authenticated using a short tandem repeat analysis kit, identifier (Applied Biosystems, Foster City, CA), as directed at the Johns Hopkins Genetic Resources Core Facility. The results were shown in Supplementary Table II. Cell growth conditions were maintained at 37°C in an atmosphere of 5% CO<sub>2</sub>.

### Transient Transfection, *NOTCH* inhibition and Cell Proliferation Assay

ON-TARGETplus Pool of siRNAs against *NOTCH1*, *HEY1* non-targeting Pool of siRNA (Thermo Scientific) was used to downregulate the expression of *NOTCH1*, *HEY1* or used as control. Cells were seeded in 96-well plates and allowed to grow until the cells were approximately 70% confluent. Cells were transfected with siRNA using Lipofectamine RNAiMAX Reagent (Invitrogen). *NOTCH1* was inhibited by Gamma Secretase Inhibitor XXI, Compound E (GSI-XXI, EMD Millipore). Cell metabolic activity was determined every 24 hours using the CCK-8 colorimetric assay (Dojindo). Values are mean  $\pm$  SEM for pentaplicates of cultured cells. The transfection efficiency was confirmed by qRT-PCR as described above for primary tissues with primers and probes for *NOTCH1*, or *HEY1* and normalized to *GAPDH* at 48 hours time point.

### Analysis of the TCGA HNSCC Data

The TCGA datasets, including DNA copy number datasets from 288 HNSCC tumor tissues, RNA-seq expression datasets from 279 HNSCC tumor tissues and 37 adjacent normal tissues, and *NOTCH1* mutation data sets from 281 HNSCC tumor tissues, were obtained from the public access data portal (32). The DNA copy number, RNA expression, and *NOTCH1* mutation in HNSCCs were assayed using Affymetrix 6.0 SNP arrays, RNAseq, and Whole genome sequencing respectively. Among these data sets, 279 HNSCC tumor tissues had full DNA copy number, RNA-seq expression, and *NOTCH1* mutation data available, and hereby were used in our study.

### Statistical Analysis

All RT-PCR analyses utilized an unpaired Student's t test to determine statistical significance between experimental variables. All statistical tests were two sided without

multiple testing correction. A  $p$  value threshold of  $\alpha = 0.05$  was used to indicate statistical significance. All computations were done in R 2.15.2.

## Results

### DNA Copy Number and promoter methylation analysis of *NOTCH* signaling pathway genes in HNSCC vs normal mucosa

Recently, our laboratory and others have reported that *NOTCH1* is a putative tumor suppressor gene mutated and inactivated at a significant frequency (~15%) in HNSCC (7). *NOTCH1* encodes a member of *NOTCH* signaling pathway, a pathway comprised of 47 genes according to the KEGG database annotation (Supplementary Table III). The goal of this study was to explore the comprehensive alterations of *NOTCH* signaling pathway in HNSCC and their potential involvement in HNSCC development. To achieve this goal, we analyzed the DNA copy number, methylation and expression array data generated from 44 HNSCC tumor tissues and 25 normal mucosa tissues in our laboratory. The microarray data was uploaded to GEO with an accession number “33205”. The demographic and clinical characteristics of this cohort are presented in Supplementary Table I.

We firstly performed DNA copy number array data analysis on 38 of the 47 *NOTCH* signaling pathway genes from the above cohort, as these genes had data available on Affymetrix SNP 6.0 arrays. Outlier sums were used to identify those *NOTCH* signaling pathway genes with significant copy number gains, highlighting 8 *NOTCH* signaling pathway genes, including *NOTCH* ligand *JAG1* ( $P=0.040$ ), *MAML2* ( $P=0.026$ ), *MAML3* ( $P=0.006$ ), *NCOR2* ( $P=0.003$ ), *NUMB* ( $P=0.039$ ), *NUMBL* ( $P=0.020$ ), *PSEN1* ( $P=0.010$ ), and *NSCTN* ( $P=0.049$ ) (Figure 1A). Our analysis identified a number of samples exhibiting copy number gains in one or more of these 8 genes. These comprised 5, 5, 5, 9, 6, 4, 7, and 6 out of the 44 HNSCC tumors for copy number gains of *JAG1*, *MAML2*, *MAML3*, *NCOR2*, *NUMB*, *NUMBL*, *PSEN1*, and *NSCTC*, respectively (Figure 1A and 1B).

We then analyzed the promoter methylation status of *NOTCH* signaling pathway genes using the DNA methylation array data from the cohort of 44 HNSCC tumor tissues and 25 normal mucosal tissues. Preliminary analysis was conducted using the 12, 023 probes on the arrays that included 3 CpG islands probe using empirical Bayes comparisons for all tissue types. Given that we were interested in *NOTCH* pathway genes that are promoter hypomethylated and overexpressed in HNSCC tumors, the outlier sums were applied in the analysis to identify those *NOTCH* pathways exhibiting left-tail outliers, indicating promoter hypomethylation in HNSCC tumors in comparison to that in normal mucosa. With this analysis, we found none of the *NOTCH* pathway genes is significantly promoter hypomethylated in HNSCC tumors versus normal mucosa. However, *PSEN2* and *PSENE1* trended toward promoter hypomethylation with  $p$ -values of 0.052 and 0.072 respectively (data not shown).

### Gene Expression Analysis of *NOTCH* signaling pathway genes in HNSCC tumors vs normal mucosa

We then extended our analysis on the transcriptional levels of the *NOTCH* pathway genes using the expression array data from the same cohort described above. Forty-three of the 47 *NOTCH* pathway genes illustrated by KEGG database are available on the Affymetrix HuEx 1.0 GeneChip (Supplementary Table III). When the differential expression of these individual genes was analyzed, we found 15 genes showing a significant differential expression ( $P<0.05$ ). Among the 15 genes, the mRNA levels of *JAG1*, *JAG2*, *NOTCH3*, *NCSTN*, *ADAM17*, *DTX3L*, *DVL3*, *HES1*, *HDAC2*, *NCOR2*, and *NUMBL* were significantly higher in primary HNSCC tumors than in normal mucosa whereas the mRNA levels of

*KAT2B*, *MAML3*, *DTX1* and *MFNG* significantly lower in HNSCC tumors than in normal mucosa (Supplementary Table IV). Of note, *JAG1* and *JAG2* ligands and *NOTCH3* receptor were among the *NOTCH* pathway genes significantly overexpressed in tumors (*JAG1*, log<sub>2</sub> mean, 9.4; *JAG2*, log<sub>2</sub> mean, 7.9; *NOTCH3*, log<sub>2</sub> mean, 8.3) compared to those in normal mucosa (*JAG1*, log<sub>2</sub> mean, 8.5,  $P < 0.001$ ; *JAG2*, log<sub>2</sub> mean, 7.4,  $P < 0.001$ ; *NOTCH3*, log<sub>2</sub> mean, 8.0,  $P = 0.007$ ) (Figure 2A).

We constructed a heat map depicting the differential expression of the *NOTCH* Signaling pathway genes in the cohort of 44 HNSCC tumors and 25 normal mucosa (Figure 2B). Importantly, we found 29.5% (13/44), 34.1% (15/44), and 18.2% (8/44) of HNSCC tumors showed overexpression of *JAG1*, *JAG2*, and *NOTCH3* when compared with the normal mucosa. Of note, in our gene-set analysis, we observed a marginal statistical trend ( $P = 0.067$ ) that *NOTCH* signaling pathway genes tended to be differentially expressed. We also found that there was significant differential expression of the gene set of Nguyen\_ *NOTCH1*\_Targets ( $P < 0.001$ ) in the HNSCC tumor cohort, suggesting that *NOTCH* signaling pathway is dysregulated on a pathway basis in HNSCC. Of note, the value of the Nguyen\_ *NOTCH1*\_Targets set in evaluation of the *NOTCH* signaling pathway status in HNSCC tumors may be limited, given that the gene set was identified in primary keratinocytes and that it may differ from the *NOTCH* downstream targets in HNSCCs.

In addition, we compared the gene expression levels of the eight *NOTCH* pathway genes (exhibiting copy number gains; Figure 1) among the tumors with increased copy number gains, the tumors without increased copy number gains, and normal tissues of our study cohort. Among these genes, our results showed the significant overexpression of *JAG1* ( $P = 0.014$ ) and *PSENI* ( $P = 0.015$ ) in the tumors with increased copy number gains in comparison to that in the normal tissues (Supplementary Figure 1).

### ***NOTCH* signaling pathway activation in HNSCC tumors**

Given the extensive *NOTCH* signaling pathway alterations identified in HNSCC tumors and in order to determine the functional status of *NOTCH* signaling, we next determined whether the *NOTCH* signaling pathway is activated in HNSCC. It is known that the *NOTCH* pathway signals through transcriptional activation of target genes, *HES1* and *HEY1*. We therefore analyzed the mRNA expression of *HES1* and *HEY1* using expression array data from the above cohort. We found that the mRNA expression of *HES1* and *HEY1* was significantly higher in HNSCC tumors than (*HES1*, log<sub>2</sub> mean, 8.1; *HEY1*, log<sub>2</sub> mean, 6.8) in normal mucosa (*HES1*, log<sub>2</sub> mean, 7.8,  $P = 0.017$ ; *HEY1*, log<sub>2</sub> mean, 6.7,  $P < 0.001$ ) (Figure 3A). Using the same threshold as defined above to declare a gene was overexpressed in an individual sample, we found that 14% (6/44) and 25% (11/44) of HNSCC tumors showed overexpression of *HES1* and *HEY1* when compared with the normal mucosa (Figure 3B). In total, we found 31.8% (14/44) of HNSCC tumors showed overexpression of *HES1* and/or *HEY1*. Given the likelihood of low expression status of *HES1* and *HEY1* as transcription factors in certain tumor samples, we also analyzed their downstream target genes as additional indicators of *HES1* or *HEY1* overexpression. Based on literature report, genes downregulated by *HES1* included *NEUROG3* (33), *GAA* (34), *CDKN1B* (35), *RCOR1* and *CFD*; genes downregulated by *HEY1*, *GATA4* and *GATA6* (36). Our results revealed that all those HNSCC tumors showing downregulation of one or more *HES1/HEY1* target genes demonstrate overexpression of *HES1* or *HEY1*. Of note, the mRNA expression of *GATA4* and *NEUROG3* were found significantly lower in HNSCC tumors with *HES1/HEY1* overexpression compared with those HNSCC tumors without *HES1/HEY1* overexpression ( $P = 0.008$ ) and compared with normal mucosa ( $P = 0.02$ ), respectively; The mRNA expression of *NEUROG3* showed significant downregulation in HNSCC tumors with *HES1/HEY1* overexpression compared to those HNSCC tumors without *HES1/HEY1*

overexpression and showed a trend toward downregulation ( $P=0.03$ ) when compared with the normal mucosa ( $P=0.067$ ) (Figure 3C). Taken together, these results suggested that *NOTCH* signaling pathway is activated in 31.8% of HNSCC tumors.

In addition, to compare the pattern and intensity of HES1/HEY1 in tumor versus normal epithelium and correlate these with NOTCH1 at the protein levels, we constructed a tissue microarray comprising 56 primary HNSCC and 11 normal control mucosa, and performed immunohistochemistry analysis using commercially available antibody for HES1, HEY1, as well as activated NOTCH1. Due to the availability of the samples, we were able to include 5 HNSCC tumors on the tissue microarrays that originated from the same HNSCC cohort used for our microarray genomic analysis. The patient demographic and clinical variables were similar to the original 44 tumors and 25 normal tissues. Our results showed that 1) NOTCH1 protein is significantly overexpressed in tumor samples, as compared to normal tissues ( $P=0.02$ ); 2) HES1 and HEY1 were overexpressed in 17.9% (10/56) and 14.3% (8/56) tumor samples; either HES1 or HEY1 were overexpressed in 26.8% (15/56) of HNSCC samples which is comparable to that in our expression array data (31.8%); 3) 10 HNSCC tumors with elevated levels of NOTCH1 have overexpressed HES1 or HEY1; 4) among the five tumor samples originating from the same patient samples used for our microarray analysis, two (X7 and X11) demonstrated strong correlation of RNA and protein for HES1, HEY1 and NOTCH1 expression (Supplementary Figure 2).

#### **Quantitative RTPCR Validation of *NOTCH* ligand, receptor, and target overexpression *HES1*, *HEY1* in primary HNSCC**

To validate the reliability of *HES1* and *HEY1* overexpression as assessed by expression microarrays in the cohort of 44 HNSCC tumors and 25 normal mucosa, we performed quantitative RT-PCR analysis on the same cohort. Our quantitative RT-PCR results confirmed the significant overexpression of *HES1* and *HEY1* in HNSCC tumors versus normal mucosa. The mean log<sub>10</sub> mRNA levels for *HES1* and *HEY1* in primary HNSCCs were 1.1 (log<sub>10</sub> range, 0.4 to 2.0) and 1.0 (log<sub>10</sub> range, 0.1 to 1.8); in normal mucosa, the mean log<sub>10</sub> mRNA levels for *HES1* and *HEY1* were 0.8 (log<sub>10</sub> range, 0.1 to 1.4,  $P=0.013$ ) and 0.8 (log<sub>10</sub> range, 0.4 to 1.1,  $P=0.043$ ), showing that Hes1 and Hey1 was significantly overexpressed (Figure 4A).

We further validated the overexpression of *HES1* and *HEY1* in an independent HNSCC cohort with 31 HNSCC tumors and 17 normal mucosa in non-cancer controls by quantitative RT-PCR. As expected, significantly increased expression levels of Hes1 and Hey1 were found in HNSCC (*HES1*, log<sub>10</sub> mean, 1.0; *HEY1*, log<sub>10</sub> mean, 0.9) versus normal mucosal tissues (*HES1*, log<sub>10</sub> mean, 0.7,  $P<0.01$ ; *HEY1*, log<sub>10</sub> mean, 0.5,  $P<0.01$ ) (Figure 4B). We also validated the overexpression of *JAG1* in this independent cohort. Our quantitative RT-PCR assay showed significantly increased levels of *JAG1* expression in HNSCC tumor tissues (log<sub>10</sub> mean, 1.1) in comparison with normal mucosa (log<sub>10</sub> mean, 0.6,  $P<0.001$ ) (Figure 4C). Further, we validated the overexpression *JAG2* in a cohort of 63 HNSCC tumors vs 30 normal mucosa. The mRNA levels of *JAG2* were significantly increased in HNSCC tumors (log<sub>10</sub> mean, 1.1) in comparison with that in normal mucosa (log<sub>10</sub> mean, 0.9,  $P<0.001$ ) (Figure 4D). The application of different cohorts for quantitative RTPCR validation showing similar alterations validates the initial findings in our discovery cohort.

#### **A subset of wildtype *NOTCH1* HNSCC tumors has increased *HES1/HEY1* expression**

To determine the potential relevance of *NOTCH1* genetic mutations to the transcriptional alterations in the *NOTCH* signaling pathway, we performed selected exome sequencing on 37 HNSCC tumors from the above cohort (6 samples including X14, X15, X20, X26, X30 and X37 were eliminated for sequencing due to inadequate DNA; an additional sample X3



was eliminated for not passing quality control criteria) and their paired normal lymphocytes. A total of 5 *NOTCH1* mutations were identified in 4 of 37 (10.8%) HNSCC tumors. Consistent with our previous study, next to TP53, *NOTCH1* was found the most frequently mutated gene found in the 37 HNSCC tumors (Figure 5A). Also the *NOTCH1* mutation rate in this study was found similar to that in our former reported cohort. Four of the *NOTCH1* mutations were predicted to truncate the protein product, whereas 1 was missense. Among the four nonsense mutations (R56\*, Q154\*, E1294\*, W1843\*), one mutation of W1843\* was clustered in the RBP-Jk-associated module (RAM) domain, whereas the other 3 mutations next to or in the N-terminal epidermal growth factor (EGF)-like ligand binding domain. Similarly, the 1 missense mutation (T1138I) was also clustered in the N-terminal EGF-like ligand binding domain (Figure 5B). Whereas *NOTCH1* contains activating mutations in T cell acute lymphoblastic leukemia and chronic lymphocytic leukemia (mainly lying at the heterodimerization (HD) domain and C-terminal polypeptide-enriched proline, glutamate, serine, and threonine (PEST) domain of *NOTCH1*) (13), the mutations we found in the study cohort appeared to be loss-of-function mutations, consistent with those recently described in myeloid leukemia and HNSCC tumors (7, 8, 15).

We then compared downstream activation of *NOTCH* signaling pathway driven by transcriptional changes between the HNSCC tumors with and without *NOTCH1* mutations. We examined the association of *NOTCH1* mutations and *HES1/HEY1* expression status. We found the significant lower expression of *HES1* ( $P=0.013$ ) and/or *HEY1* ( $P=0.003$ ) in HNSCC tumors with mutant type *NOTCH1* than those with wild type *NOTCH1* (Figure 6A). Of note, the mRNA levels of *HES1* ( $P=0.104$ ) or *HEY1* ( $P=0.970$ ) in HNSCC tumors with *NOTCH1* mutant were similar to those in the normal mucosa, and none of these 4 HNSCC tumors with *NOTCH1* mutant exhibited *HES1/HEY1* overexpression, consistent with the loss-of-function of *NOTCH1* mutations described above. Intriguingly, we found that among the 33 HNSCC tumors with wild type status, 10 (30.3%, 10/33) exhibited *HES1/HEY1* overexpression, implicating *NOTCH* pathway activation in these HNSCC tumors. Thus, by comparison of the pattern of copy number alteration, transcriptional alteration and downstream activation of *NOTCH* pathway activation in wildtype *NOTCH1* tumors, we found in the wildtype *NOTCH1* HNSCC tumors there exist a group of *NOTCH1* pathway activated HNSCC tumors (Figure 6B).

In the 44 HNSCC from our initial study cohort, 13 were HPV-positive. We hereby determined the association between HPV status and *NOTCH1* mutation status, as well as the mRNA levels of *HES1* and *HEY1*. We found that the association between HPV status and *NOTCH1* status was not statistically significant ( $P=0.55$ , Fisher's exact test); No statistically significant differences in mRNA levels of *HES1* ( $P=0.37$ , student's t test) and *HEY1* ( $P=0.96$ , student's t test) between HPV-positive and HPV-negative HNSCC tumors were observed (data not shown). Therefore, we did not perform the *NOTCH* signaling pathway analyses in HPV-positive or HPV-negative tumors separately in this study.

### **The subset of wild-type *NOTCH1* HNSCC tumors with increased *HES1/HEY1* expression is validated in TCGA HNSCC cohort**

To validate the pattern of *NOTCH1* pathway alterations revealed in our HNSCC cohort, we further analyzed the available *NOTCH1* mutation, copy number, and expression data of *NOTCH* pathway in the TCGA HNSCC cohort (including *NOTCH1* mutation, copy number and expression data sets from 279 HNSCC tumors and expression data set from 37 adjacent normal tissues). Similar to the alterations revealed in our initial HNSCC cohorts, increased expression of *JAG1* ( $P<0.001$ ), *JAG2* ( $P<0.001$ ) and *NOTCH3* ( $P=0.004$ ) were found in HNSCC tumors vs adjacent normal tissues in the TCGA HNSCC cohort (Supplementary Figure 3A). The significant overexpression of *JAG1* ( $P<0.001$ ) and *PSEN1* ( $P<0.001$ ) in

HNSCC tumors with increased copy number gains compared with that in normal tissues were also validated in the TCGA HNSCC cohort. Moreover, in the TCGA HNSCC cohort, we found that *JAG1* and *PSEN1* were overexpressed in the tumors with increased copy number gains in comparison to those tumors without increased copy number gains. (Supplementary Figure 3B).

In the TCGA cohort, a total of 67 mutations in *NOTCH1*, comprised of 14 frame shift dels, 1 in frame del, 51 nonsense mutations, and 1 splice site-associated mutation, were found in 52 HNSCC tumors. We observed that decreased expression of *HES1* had a borderline significance ( $P=0.064$ ) in *NOTCH1* mutant type vs wild type HNSCC tumors whereas increased expression of *HEY1* has a statistically significant difference ( $P=0.012$ ) (Figure 7A). It should be of note that in the TCGA HNSCC cohort, we were not able to validate the overexpression of *HES1* in HNSCC tumors vs adjacent normal tissues although a borderline significance trend was shown; this may be due to the fact that the adjacent normal tissues used in the TCGA cohort were collected from patients with HNSCC and include non mucosal tissues, whereas the normal mucosal tissues in our initial HNSCC cohort include only mucosal tissue from non-cancer patients. Accordingly, overexpression of *HEY1* instead of *HES1* was used as an indication of the *NOTCH* pathway activation in this TCGA cohort. Of interest, we found that among the 227 *NOTCH1* wild-type HNSCC tumors, 50 (22.0%) exhibited overexpression of *HEY1*, confirming a subset of *NOTCH* pathway activation, wild-type *NOTCH1* HNSCC primary tumors (Figure 7B).

To test the feasibility of the *NOTCH* pathway as target for future directed therapy, we explored the functional consequences when *NOTCH1* is inhibited by siRNA in *NOTCH1* wildtype cells (090 and SCC61). As shown in Supplementary Figure 4, following transfection with *NOTCH1* siRNAs, *NOTCH1* wildtype 090 and SCC61 cells showed dramatic and modest decrease in cell proliferation respectively. To validate the different functional consequences mediated by inhibition with *NOTCH1* siRNAs in *NOTCH1* wildtype cells, we then examined the growth effects upon siRNA inhibition of *HEY1*. Consistent with the results showing by siRNA inhibition of *NOTCH1*, we noted a significant decrease of cell growth in *NOTCH1* wildtype 090 cells inhibited with *HEY1* siRNAs (Supplementary Figure 5). Similarly, when *NOTCH* pathway inhibitor GSI-XXI was applied, the cell growth in *NOTCH1* wildtype 090 cells was modestly inhibited (Supplementary Figure 6).

## Discussion

The *NOTCH* signaling pathway regulates many facets of cancer biology, including stem cell renewal, proliferation, tumor angiogenesis, and metastasis (37). The *NOTCH* signaling pathway has been implicated in the tumorigenesis of several solid tumor malignancies including, but not limited to, non-small cell lung adenocarcinoma (38), melanoma, and ovarian carcinoma (39). However, the molecular alterations of the *NOTCH* signaling pathway in HNSCC are less well defined. We have previously reported that *NOTCH1* mutations occur in ~15% of HNSCC patients, implicating a critical role of *NOTCH* signaling pathways in HNSCC tumors (7). Here we extend our study to analyze the comprehensive molecular alterations of *NOTCH* signaling pathway genes and the *NOTCH* signaling pathway downstream activation status in HNSCC tumors. To better define the alterations of *NOTCH* signaling pathway, we have conducted DNA copy number, methylation, expression and mutation analysis from a cohort of 44 HNSCC tumors and 25 normal mucosa.

Our data demonstrate the frequent occurrence of aberrant DNA copy number gains of *NOTCH* signaling pathway genes in HNSCC tumors compared to that in normal mucosa.

We reported that 8 *NOTCH* pathway genes exhibited increased DNA copy numbers in HNSCC tumors versus normal mucosa based on outlier analysis. We observed that there are outlier HNSCC tumors with copy number gains of these *NOTCH* pathway genes. The broad copy number alterations identified in this study imply that in addition to *NOTCH1* mutations, copy number gains of *NOTCH* signaling pathway genes may contribute to HNSCC tumor development. Among these genes featuring copy number gains in HNSCC tumors, the identification of *NOTCH* ligand *JAG1* is intriguing. In support of the findings of the copy number increase of *JAG1* in this study, previously studies from our laboratory and others using SNP6.0 microarrays or high-resolution microarray comparative genomic hybridization showed that chromosome 20p, a region containing *JAG1*, is amplified at high frequency in HNSCC tumors (40). Moreover, our expression array analysis demonstrated that *JAG1* was significantly overexpressed (30%) in HNSCC tumors compared to that in normal mucosa. Our study suggests that genomic amplification in part contributes to the overexpression of *JAG1* in HNSCC (Pearson correlation coefficient between copy number levels and mRNA expression: 0.6, data not shown). Recently, studies on the function significance of *JAG1* in cancer development have been published. For example, the upregulation of *JAG1* in breast cancer has been implicated metastatic disease and correlated with poor prognosis (41) and *JAG1* plays a critical role in the promotion of bone metastatic outgrowth of breast cancer (11). In addition, we note that 4 out of 5 patients with *JAG1* gains also have a gain in either *NUMB* or *NUMBL*, which are known inhibitors of the *NOTCH* pathway. In this respect, it remains unclear whether expressing the *NOTCH* ligand *JAG1* and *NOTCH* regulating genes such as *NUMB* and *NUMBL* within the same tumors would actually contribute to *NOTCH* signaling or instead result in cis-inhibition of the pathway.

To identify the potential epigenetic alterations of *NOTCH* signaling pathway genes, in particular promoter methylation in HNSCC tumors, we performed methylation analysis using Illumina's Infinium methylation data generated from the above cohort. We report that none of the *NOTCH* pathway genes present in on the methylation array exhibit promoter hypomethylation in HNSCC tumors compared with that in normal mucosa although two genes (*PSEN2* and *PSENSEN*) with borderline significance were noted, implicating that methylation alterations may play a less common role in regulating Notch pathway genes during HNSCC tumor development.

We next examined the transcriptional alterations of *NOTCH* signaling pathway genes in HNSCC tumors using the expression array data from the cohort of 44 HNSCC tumors and 25 normal mucosa. These include genes involved in the molecular and biochemical events occur during of ligand-receptor recognition, receptor activation, intramembrane proteolysis, and target gene selection (42). Our result revealed that 11 genes, including *JAG1*, *JAG2*, *NOTCH3*, *NCSTN*, *DTX3L*, *ADAM17*, *DVL3*, *HES1*, *HDAC2*, *NCOR2* and *NUMBL*, were significantly upregulated, and 4, including *KAT2B*, *MAML3*, *DTX1* and *MFNG*, were downregulated. Of the overexpressed genes, *JAG2* was found to promote lung adenocarcinoma metastasis through a miR-200-dependent pathway in mice (43). In nasopharyngeal carcinoma, Man CH et al's studies indicate that activation of *NOTCH3* pathway is a critical oncogenic event in nasopharyngeal carcinoma development (44). *NCSTN*, encoding a  $\gamma$ -secretase component, was recently shown to be a potential driver gene in human liver carcinoma by genome wide screening (45). *DTX3L*, a member of the deltex family of proteins that function as E3 ligases and modify *NOTCH* signaling, has been shown amplification and overexpression in cervical cancer (46); and consistent with our result, *ADAM17* (*ADAM* metallopeptidase domain 17) was reported an elevated expression in malignant cells in HNSCC (47). In addition, we observed a marginal statistical trend that *NOTCH* pathway genes tend to be differentially expressed. Taken together, these results

suggest that *NOTCH* signaling pathway genes are altered at the transcriptional levels in HNSCC tumors.

Given the prevalence of the transcriptional alterations of *NOTCH* signaling pathway we observed in HNSCCs, we further investigated the activation of the *NOTCH* signaling pathway in HNSCC. To date, the best characterized gene targets indicating *NOTCH* signaling pathway activation are members of the hairy and enhancer of split (HES) and the Hes related-repressor protein (HERP) families of bHLH transcriptional repressors such as *HES1* and *HEY1* (42, 48). In our study, we found that *HES1* and *HEY1* were significantly overexpressed in HNSCCs in comparison to that in normal mucosa. Our results revealed ~31.8% (14/44) of HNSCC tumors exhibited overexpression of *HES1* and/or *HEY1*. Notably, the overexpression of *HES1* and/or *HEY1* was supported by the downregulation of their downstream responsive genes. The findings that *HES1* and *HEY1* were overexpressed in our HNSCC cohort shown in expression microarray were also validated by quantitative real-time RTPCR analysis in the same HNSCC cohort as well as an additional validation cohort. In addition, we found a significant differential expression of Nguyen\_*NOTCH1*\_Target gene set (differentially expressed genes concomitantly modulated by activated *NOTCH1* in mouse and human primary keratinocytes) in 44 HNSCC tumor tissues (28). Although the estimating power of Nguyen gene set in evaluated the *NOTCH* signaling pathway status maybe moderate given the evidence that this gene set originated from primary keratinocyte rather than head and neck epithelial cells, this result support the notion that *NOTCH* signaling pathway is dysregulated in HNSCCs.

To gain a more complete understanding of the *NOTCH1* mutations relevant to the transcriptional alterations of *NOTCH* signaling pathway and to the *NOTCH* signaling pathway activation, we performed selected exome sequencing using the massive parallel next generation sequencing techniques on 37 HNSCC tumors used for the above microarray expression analysis. We observed 5 *NOTCH1* mutations occurring in ~10.8% (4/37) HNSCC tumors. Of these *NOTCH1* mutations, 4 predicted to result in loss of the majority of amino acids from the translated protein; the remaining 1 missense mutation located in N-terminal EGF-like ligand-binding domain. A dual biological of *NOTCH1* as either cancer promoting or tumor suppressing has been highlighted. It is reported that gain-of-function *NOTCH1* mutations found in leukemia's cluster in the negative regulatory region and the C-terminal PEST domain (13), whereas the loss-of-function *NOTCH* mutations in cutaneous and lung squamous cell carcinoma span ectodomain and the N-terminal portion of the intracellular domains that include nonsense mutations leading to receptor truncations (14). Thus it is likely that gain- and loss-of-function mutations occur at different regions of the *NOTCH1* gene. Our and others' study of sequence analysis and in HNSCC tumors demonstrated that that the majority of *NOTCH1* mutations in HNSCC affect either the EGF-like ligand-binding domain or the NICD domain, suggesting loss of function (7, 8). Our data support the notion that the *NOTCH1* mutations found in this study are loss-of-function mutations and play a tumor-suppressive role during HNSCC development.

Moreover, our result showed that the HNSCC tumors with *NOTCH1* mutation exhibited decreased *HES1/HEY1* expression in comparison to that in HNSCC tumors with *NOTCH1* wild type. However, we reported that the mRNA levels of *HES1/HEY1* in HNSCC tumors with *NOTCH1* mutant is similar to that in the normal mucosa and overexpression of *HES1/HEY1* was found in none of the HNSCC tumors with *NOTCH1* mutant. This data is in agreement with a lack of *NOTCH* activation in *NOTCH1* mutant HNSCC tumors. It is notable that, although the absence of elevated *HES1/HEY1* correlated with *NOTCH1* mutations, these 4 patient samples also appear to have lower *NOTCH3* compared to many of the samples.

Interestingly, our data also suggest that a large subset of HNSCC tumors with *NOTCH1* wild type sequence exhibit *NOTCH* pathway copy number increase, increased expression and downstream activation (Figure 6 and Figure 7). In our HNSCC initial cohort, a subset of *NOTCH1* wild type (~30.3%) HNSCC tumors had *HES1/HEY1* overexpression (downstream activation). This subset of HNSCC tumors featuring wild type *NOTCH1* status and *HES1/HEY1* overexpression was also validated in TCGA HNSCC cohort. In support of this notion, our initial functional results showed that in the *NOTCH1* wildtype 090 HNSCC cells, siRNA inhibition of *NOTCH1* or *HEY1* significantly decreased cell growth; and the application of GSI-XXI, a *NOTCH* pathway inhibitor to 090 HNSCC cells also inhibited cell growth. It is possible that one explanation for the the differential response of two wildtype cell lines (090 and SCC61) to *NOTCH* pathway inhibition may be the presence of HPV (090, HPV positive; SCC61, HPV negative), however, other concurrent pathway alterations may also explain this response.

In summary, the present study demonstrated systematic transcriptional alterations of *NOTCH* signaling pathway in HNSCC tumors by using a large cohort comprised of HNSCC tumors and normal mucosas. The study provides strong evidence supporting the prevalent activation of *NOTCH* signaling pathway in HNSCC tumors and an overall bimodal pattern in HNSCC. In HNSCC tumors with *NOTCH1* mutant, there is a lack of *NOTCH* pathway activation due to the loss-of-function mutations; whereas in HNSCC tumors with *NOTCH1* wild type, there is a larger subset of HNSCC tumors exhibit ligand receptor copy number increase, increased expression and downstream pathway activation. Our studies may suggest that in a subset of HNSCC tumors, the *NOTCH* pathway may be driving the growth is a potential therapeutic target; yet it is unclear if in other HNSCC tumors, the signaling may actually impair the growth of wildtype tumors to some degree. The findings reported in the present study may have important implications for development of *NOTCH* pathway targeting therapies, in particular for those *NOTCH* wildtype, *NOTCH* pathway activated HNSCC tumors that may be targeted by *NOTCH* inhibiting therapies.

## Supplementary Material

Refer to Web version on PubMed Central for supplementary material.

## Acknowledgments

**Grant Support:** The work was supported by National Institute of Dental and Craniofacial Research (NIDCR) and NIH Challenge Grant RC1DE020324 and RC2DE020789, and NCI P50 DE 019032 Head and Neck Cancer SPORE.

The manuscript/analysis of this article is based on a web database application provided by Research Information Technology Systems (RITS)—<https://www.rits.onc.jhmi.edu/>.

## References

1. Leemans CR, Braakhuis BJ, Brakenhoff RH. The molecular biology of head and neck cancer. *Nature reviews Cancer*. 2011; 11:9–22.
2. Poeta ML, Manola J, Goldenberg D, Forastiere A, Califano JA, Ridge JA, et al. The Ligamp TP53 Assay for Detection of Minimal Residual Disease in Head and Neck Squamous Cell Carcinoma Surgical Margins. *Clin Cancer Res*. 2009; 15:7658–65. [PubMed: 19996217]
3. Demokan S, Chuang A, Suoglu Y, Ulsan M, Yalniz Z, Califano JA, et al. Promoter methylation and loss of p16(INK4a) gene expression in head and neck cancer. *Head Neck*. 34:1470–5. [PubMed: 22106032]
4. Papadimitrakopoulou VA, Izzo J, Mao L, Keck J, Hamilton D, Shin DM, et al. Cyclin D1 and p16 alterations in advanced premalignant lesions of the upper aerodigestive tract: role in response to

- chemoprevention and cancer development. *Clin Cancer Res.* 2001; 7:3127–34. [PubMed: 11595705]
5. Murugan AK, Hong NT, Fukui Y, Munirajan AK, Tsuchida N. Oncogenic mutations of the PIK3CA gene in head and neck squamous cell carcinomas. *International journal of oncology.* 2008; 32:101–11. [PubMed: 18097548]
  6. Bonner JA, Harari PM, Giralt J, Cohen RB, Jones CU, Sur RK, et al. Radiotherapy plus cetuximab for locoregionally advanced head and neck cancer: 5-year survival data from a phase 3 randomised trial, and relation between cetuximab-induced rash and survival. *Lancet Oncol.* 11:21–8. [PubMed: 19897418]
  7. Agrawal N, Frederick MJ, Pickering CR, Bettegowda C, Chang K, Li RJ, et al. Exome sequencing of head and neck squamous cell carcinoma reveals inactivating mutations in NOTCH1. *Science.* 333:1154–7. [PubMed: 21798897]
  8. Stransky N, Egloff AM, Tward AD, Kostic AD, Cibulskis K, Sivachenko A, et al. The mutational landscape of head and neck squamous cell carcinoma. *Science.* 2011; 333:1157–60. [PubMed: 21798893]
  9. Pickering CR, Zhang J, Yoo SY, Bengtsson L, Moorthy S, Neskey DM, et al. Integrative genomic characterization of oral squamous cell carcinoma identifies frequent somatic drivers. *Cancer discovery.* 2013
  10. Kalaitzidis D, Armstrong SA. Cancer: The flipside of Notch. *Nature.* 473:159–60. [PubMed: 21562551]
  11. Sethi N, Dai X, Winter CG, Kang Y. Tumor-derived JAGGED1 promotes osteolytic bone metastasis of breast cancer by engaging notch signaling in bone cells. *Cancer Cell.* 19:192–205. [PubMed: 21295524]
  12. Puente XS, Pinyol M, Quesada V, Conde L, Ordonez GR, Villamor N, et al. Whole-genome sequencing identifies recurrent mutations in chronic lymphocytic leukaemia. *Nature.* 2011; 475:101–5. [PubMed: 21642962]
  13. Weng AP, Ferrando AA, Lee W, Morris JPt, Silverman LB, Sanchez-Irizarry C, et al. Activating mutations of NOTCH1 in human T cell acute lymphoblastic leukemia. *Science.* 2004; 306:269–71. [PubMed: 15472075]
  14. Wang NJ, Sanborn Z, Arnett KL, Bayston LJ, Liao W, Proby CM, et al. Loss-of-function mutations in Notch receptors in cutaneous and lung squamous cell carcinoma. *Proceedings of the National Academy of Sciences of the United States of America.* 2011; 108:17761–6. [PubMed: 22006338]
  15. Klinakis A, Lobry C, Abdel-Wahab O, Oh P, Haeno H, Buonamici S, et al. A novel tumour-suppressor function for the Notch pathway in myeloid leukaemia. *Nature.* 2011; 473:230–3. [PubMed: 21562564]
  16. Hammerman PS, Hayes DN, Wilkerson MD, Schultz N, Bose R, Chu A, et al. Comprehensive genomic characterization of squamous cell lung cancers. *Nature.* 2012; 489:519–25. [PubMed: 22960745]
  17. Sun W, Zaboli D, Wang H, Liu Y, Arnaoutakis D, Khan T, et al. Detection of TIMP3 promoter hypermethylation in salivary rinse as an independent predictor of local recurrence-free survival in head and neck cancer. *Clin Cancer Res.* 18:1082–91. [PubMed: 22228635]
  18. Carvalho AL, Henrique R, Jeronimo C, Nayak CS, Reddy AN, Hoque MO, et al. Detection of promoter hypermethylation in salivary rinses as a biomarker for head and neck squamous cell carcinoma surveillance. *Clinical cancer research: an official journal of the American Association for Cancer Research.* 2011; 17:4782–9. [PubMed: 21628494]
  19. Scharpf RB, Irizarry RA, Ritchie ME, Carvalho B, Ruczinski I. Using the R Package crlmm for Genotyping and Copy Number Estimation. *J Stat Softw.* 2011; 40:1–32. [PubMed: 22523482]
  20. Tibshirani R, Hastie T. Outlier sums for differential gene expression analysis. *Biostatistics (Oxford, England).* 2007; 8:2–8.
  21. Phipson B, Smyth GK. Permutation P-values should never be zero: calculating exact P-values when permutations are randomly drawn. *Stat Appl Genet Mol Biol.* 2010; 9:Article39. [PubMed: 21044043]

22. Kanehisa M, Goto S, Kawashima S, Okuno Y, Hattori M. The KEGG resource for deciphering the genome. *Nucleic acids research*. 2004; 32:D277–80. [PubMed: 14681412]
23. Carvalho BS, Irizarry RA. A framework for oligonucleotide microarray preprocessing. *Bioinformatics*. 26:2363–7. [PubMed: 20688976]
24. Huber W, Gentleman R. matchprobes: a Bioconductor package for the sequence-matching of microarray probe elements. *Bioinformatics*. 2004; 20:1651–2. [PubMed: 14988118]
25. Scharpf RB, Irizarry RA, Ritchie ME, Carvalho B, Ruczinski I. Using the R Package crlmm for Genotyping and Copy Number Estimation. *J Stat Softw*. 40:1–32. [PubMed: 22523482]
26. Michaud J, Simpson KM, Escher R, Buchet-Poyau K, Beissbarth T, Carmichael C, et al. Integrative analysis of RUNX1 downstream pathways and target genes. *BMC genomics*. 2008; 9:363. [PubMed: 18671852]
27. Smyth, GK. Limma: linear models for microarray data. In: Gentleman, R.; Dudoit, SVC.; Irizarry, R.; Huber, W., editors. *Bioinformatics and Computational Biology Solutions using R and Bioconductor*. New York: Springer; 2005. p. 397-420.
28. Nguyen BC, Lefort K, Mandinova A, Antonini D, Devgan V, Della Gatta G, et al. Cross-regulation between Notch and p63 in keratinocyte commitment to differentiation. *Genes Dev*. 2006; 20:1028–42. [PubMed: 16618808]
29. DePristo MA, Banks E, Poplin R, Garimella KV, Maguire JR, Hartl C, et al. A framework for variation discovery and genotyping using next-generation DNA sequencing data. *Nat Genet*. 43:491–8. [PubMed: 21478889]
30. McKenna A, Hanna M, Banks E, Sivachenko A, Cibulskis K, Kernytzky A, et al. The Genome Analysis Toolkit: a MapReduce framework for analyzing next-generation DNA sequencing data. *Genome Res*. 20:1297–303. [PubMed: 20644199]
31. Tewhey R, Warner JB, Nakano M, Libby B, Medkova M, David PH, et al. Microdroplet-based PCR enrichment for large-scale targeted sequencing. *Nat Biotechnol*. 2009; 27:1025–31. [PubMed: 19881494]
32. TCGA Sees Heterogeneity in Head and Neck Cancers. *Cancer Discov*. 2013; 3:475–6.
33. Lee JC, Smith SB, Watada H, Lin J, Scheel D, Wang J, et al. Regulation of the pancreatic pro-endocrine gene neurogenin3. *Diabetes*. 2001; 50:928–36. [PubMed: 11334435]
34. Yan B, Raben N, Plotz PH. Hes-1, a known transcriptional repressor, acts as a transcriptional activator for the human acid alpha-glucosidase gene in human fibroblast cells. *Biochemical and biophysical research communications*. 2002; 291:582–7. [PubMed: 11855828]
35. Murata K, Hattori M, Hirai N, Shinozuka Y, Hirata H, Kageyama R, et al. Hes1 directly controls cell proliferation through the transcriptional repression of p27Kip1. *Molecular and cellular biology*. 2005; 25:4262–71. [PubMed: 15870295]
36. Fischer A, Klattig J, Kneitz B, Diez H, Maier M, Holtmann B, et al. Hey basic helix-loop-helix transcription factors are repressors of GATA4 and GATA6 and restrict expression of the GATA target gene ANF in fetal hearts. *Molecular and cellular biology*. 2005; 25:8960–70. [PubMed: 16199874]
37. Fiuza UM, Arias AM. Cell and molecular biology of Notch. *The Journal of endocrinology*. 2007; 194:459–74. [PubMed: 17761886]
38. Dang TP, Gazdar AF, Virmani AK, Sepetavec T, Hande KR, Minna JD, et al. Chromosome 19 translocation, overexpression of Notch3, and human lung cancer. *Journal of the National Cancer Institute*. 2000; 92:1355–7. [PubMed: 10944559]
39. Bedogni B, Warneke JA, Nickoloff BJ, Giaccia AJ, Powell MB. Notch1 is an effector of Akt and hypoxia in melanoma development. *J Clin Invest*. 2008; 118:3660–70. [PubMed: 18924608]
40. Smeets SJ, Braakhuis BJ, Abbas S, Snijders PJ, Ylstra B, van de Wiel MA, et al. Genome-wide DNA copy number alterations in head and neck squamous cell carcinomas with or without oncogene-expressing human papillomavirus. *Oncogene*. 2006; 25:2558–64. [PubMed: 16314836]
41. Reedijk M, Odorcic S, Chang L, Zhang H, Miller N, McCready DR, et al. High-level coexpression of JAG1 and NOTCH1 is observed in human breast cancer and is associated with poor overall survival. *Cancer Res*. 2005; 65:8530–7. [PubMed: 16166334]
42. Kopan R, Ilagan MX. The canonical Notch signaling pathway: unfolding the activation mechanism. *Cell*. 2009; 137:216–33. [PubMed: 19379690]

43. Yang Y, Ahn YH, Gibbons DL, Zang Y, Lin W, Thilaganathan N, et al. The Notch ligand Jagged2 promotes lung adenocarcinoma metastasis through a miR-200-dependent pathway in mice. *J Clin Invest.* 2011; 121:1373–85. [PubMed: 21403400]
44. Man CH, Wei-Man Lun S, Wai-Ying Hui J, To KF, Choy KW, Wing-Hung Chan A, et al. Inhibition of NOTCH3 signalling significantly enhances sensitivity to cisplatin in EBV-associated nasopharyngeal carcinoma. *The Journal of pathology.* 2012; 226:471–81. [PubMed: 22009689]
45. Woo HG, Park ES, Lee JS, Lee YH, Ishikawa T, Kim YJ, et al. Identification of potential driver genes in human liver carcinoma by genomewide screening. *Cancer Res.* 2009; 69:4059–66. [PubMed: 19366792]
46. Wilting SM, de Wilde J, Meijer CJ, Berkhof J, Yi Y, van Wieringen WN, et al. Integrated genomic and transcriptional profiling identifies chromosomal loci with altered gene expression in cervical cancer. *Genes, chromosomes & cancer.* 2008; 47:890–905. [PubMed: 18618715]
47. Stokes A, Joutsa J, Ala-Aho R, Pitchers M, Pennington CJ, Martin C, et al. Expression profiles and clinical correlations of degradome components in the tumor microenvironment of head and neck squamous cell carcinoma. *Clin Cancer Res.* 2010; 16:2022–35. [PubMed: 20305301]
48. Iso T, Kedes L, Hamamori Y. HES and HERP families: multiple effectors of the Notch signaling pathway. *Journal of cellular physiology.* 2003; 194:237–55. [PubMed: 12548545]



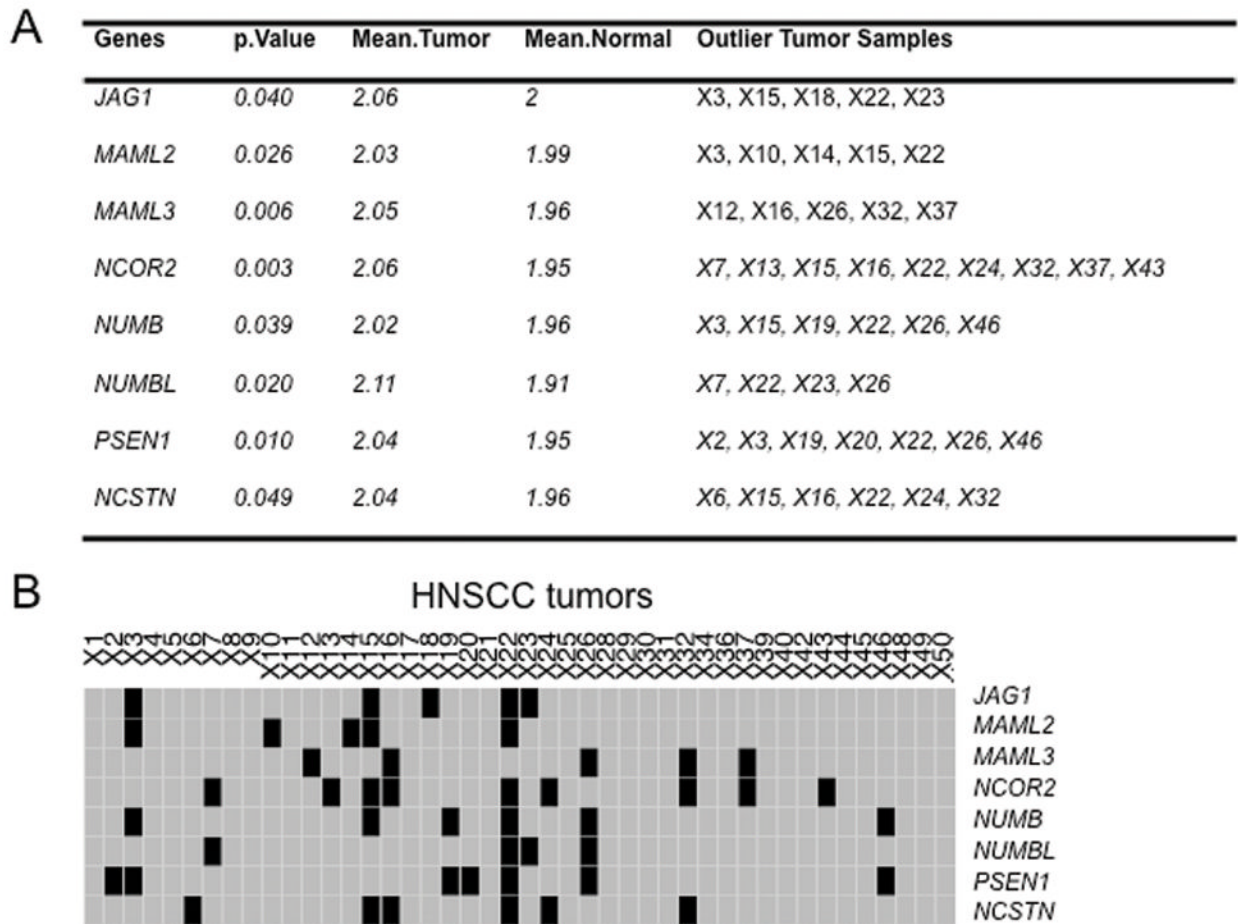


**Figure 1. Copy number analysis of *NOTCH* signaling pathway genes in the cohort of 44 HNSCC tumors and 25 normal mucosa**

**A, *NOTCH* signaling pathway genes showing significant copy number gains in HNSCC tumor tissues vs normal mucosa.** The copy number levels in 44 HNSCC tumors and 25 normal mucosa were analyzed with the Tibshirani and Hastie statistic, and the P-values were generated by permutation of sample labels to generate an empirical P-value using the approximation of Smyth and Phipson as described in methods.  $P < 0.05$  was considered significant. **B, Copy number status of the 8 *NOTCH* pathway genes in A) in the 44 HNSCC tumors.** Gray denotes no copy-number gain, Black, copy number gain and also the outlier HNSCC tumor for given gene.

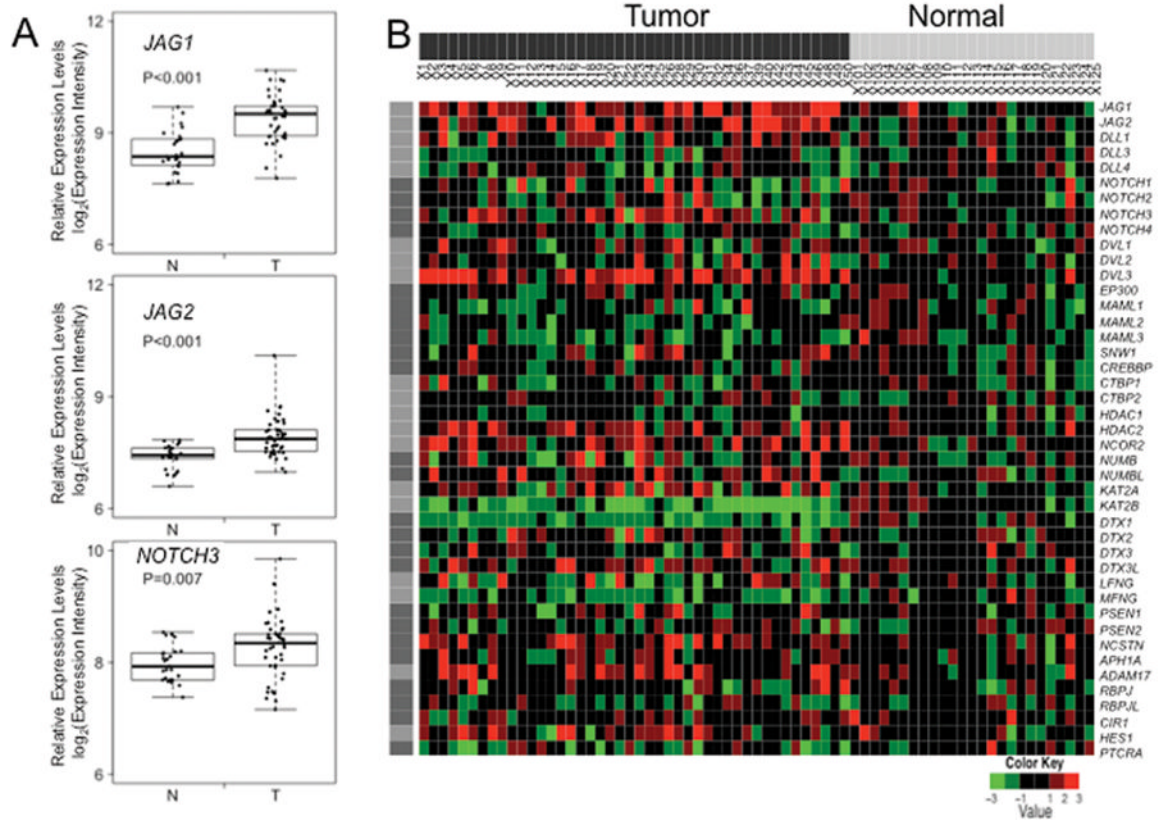


**Figure 2. Expression array analysis of *NOTCH* signaling pathway genes in the cohort of 44 HNSCC tumors and 25 normal mucosa**

**A, *JAG1*, *JAG2* and *NOTCH3* are overexpressed in HNSCC tumors vs. normal mucosa.**

Expression of *JAG1*, *JAG2*, and *NOTCH3* were assessed by Affymetrix HuEx 1.0 GeneChip platform in a cohort of 44 HNSCC tumors and 25 normal tissues. Dots, relative expression levels in different tissue samples. Boxes represent the interquartile range (25<sup>th</sup>–75<sup>th</sup> percentile) and horizontal lines inside the boxes indicate median. Whiskers indicate the minimum and maximum values. P value was calculated by using t test. N, normal mucosa; T, tumors.

**B, Heat map of gene expression of *NOTCH* signaling pathway and its downstream targets in the cohort of 44 HNSCC tumor tissues and 25 normal tissues.**

All HNSCC tumor samples are labeled black and normal tissues gray. Genes in heat map are shown in rows; each individual sample is shown in one column. For each gene, the scale bar shows color-coded differential expression from the mean gene expression level of normal tissues in standard deviation units. Red and green indicate over- or under-expression, respectively.

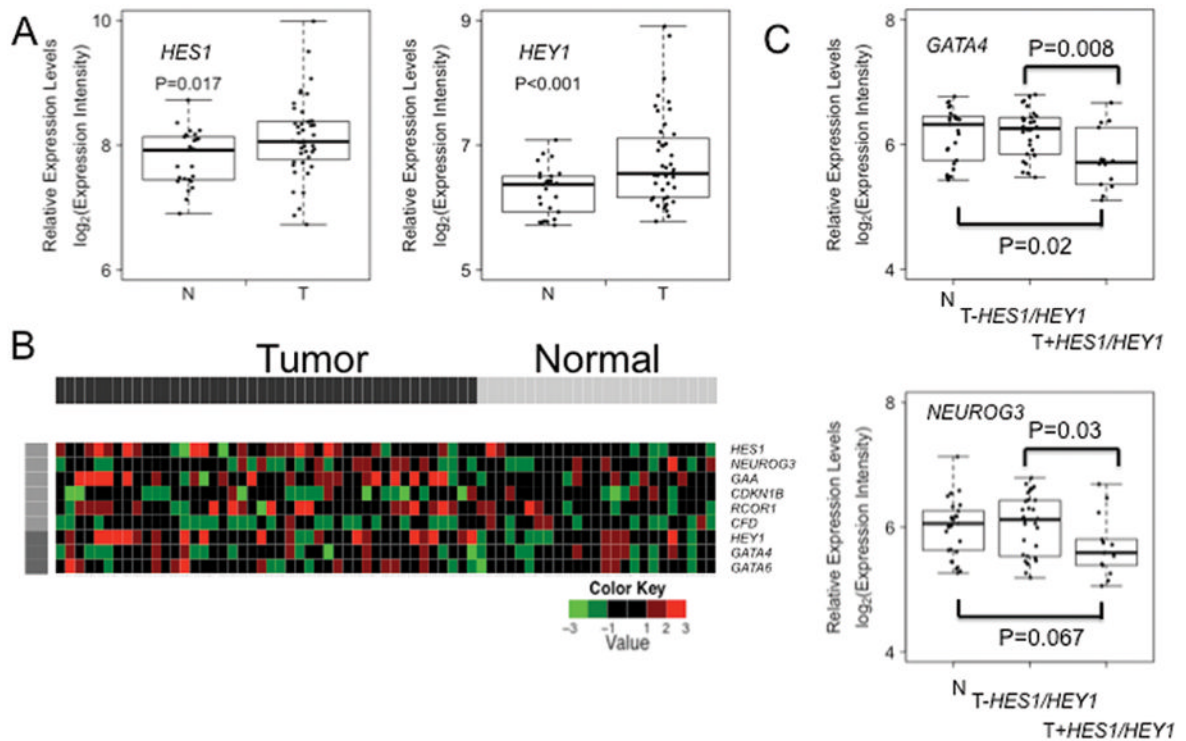


**Figure 3. Microarray Expression analysis of downstream activation of *NOTCH* signaling pathway in the cohort of 44 HNSCC tumors and 25 normal mucosa**

**A, *NOTCH* downstream targets *HES1* and *HEY1* are overexpressed in HNSCC tumors.**

Expression of *HES1* and *HEY1* were assessed by Affymetrix HuEx 1.0 GeneChip platform in a cohort of 44 HNSCC tumors and 25 normal tissues. N, normal mucosa; T, tumors.

Boxes represent the interquartile range (25<sup>th</sup>–75<sup>th</sup> percentile) and horizontal lines inside the boxes indicate median. Whiskers indicate the minimum and maximum values. P value was calculated by using t test.

**B, Heat map expression of downstream target genes (*HES1* and *HEY1*) for *NOTCH* signaling pathway in the cohort of 44 HNSCC tumor tissues and 25 normal tissues.**

As proposed by literature, expression of *NEUROG3*, *GAA*, *CDKN18*, *RCOR1*, and *CFD* are regulated by *HES1*; expression of *GATA4* and *GATA6* are regulated by *HEY1*. Thus these genes were used to assist the estimation of the *HES1/HEY1* expression.

All HNSCC tumor samples are labeled black and normal tissues gray. Genes in heat map are shown in rows; each individual sample is shown in one column. For each gene, the scale bar shows color-coded differential expression from the mean gene expression level of normal tissues in standard deviation units. Red and green indicate over- or under-expression, respectively.

**C, *GATA4* and *NEUROG3* had decreased expression in HNSCC tumors with *HES1/HEY1* overexpression in comparison to those without *HES1/HEY1* overexpression.**

N, normal mucosa; T-*HES1/HEY1*, HNSCC tumors without *HES1/HEY1* overexpression; T+*HES1/HEY1*, HNSCC tumors with *HES1/HEY1* overexpression.

Boxes represent the interquartile range (25<sup>th</sup>–75<sup>th</sup> percentile) and horizontal lines inside the boxes indicate median. Whiskers indicate the minimum and maximum values. P value was calculated by using t test.

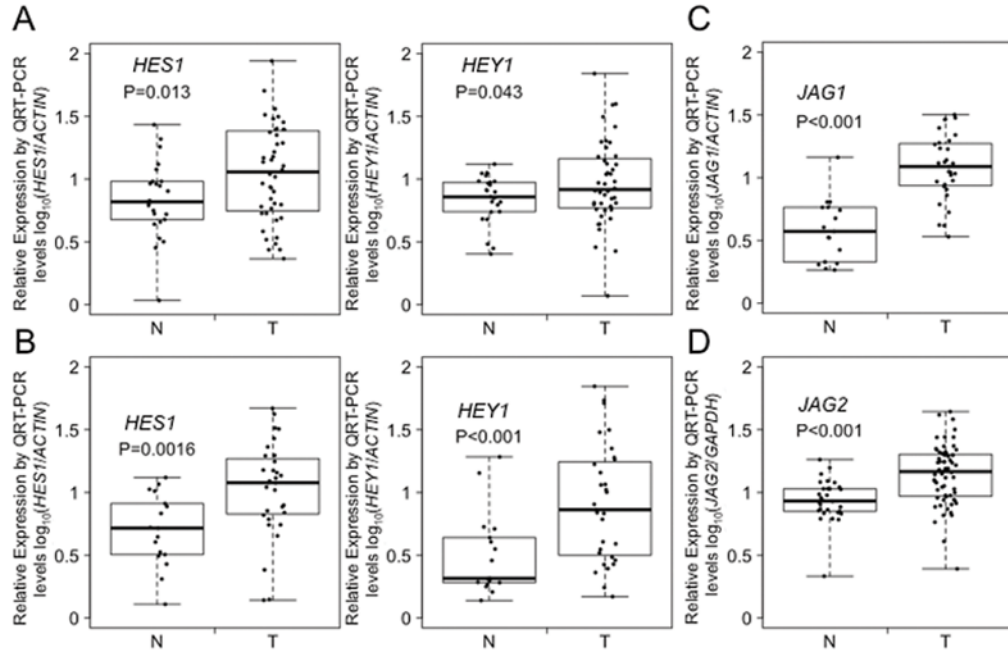


**Figure 4. Quantitative RT-PCR analysis validation of *HES1*, *HEY1*, *JAG1* and *JAG2* expression in different cohorts of HNSCC tumors and normal mucosa**  
**A, Quantitative RT-PCR analysis of *HES1* and *HEY1* expression in the original study cohort of 44 HNSCC tumors and 25 normal mucosa.** Expression of *HES1* and *HEY1* were significantly higher in HNSCC tumor tissues in comparison to normal tissues. Experiments were performed by Taqman realtime RT-PCR in triplicate and the data were normalized to *ACTIN* per sample. **B, C and D, Quantitative RT-PCR analysis of *HES1* and *HEY1* (B), and *JAG1* (C) expression in a separate cohort of 31 HNSCC tumors and 17 normal mucosa, and *JAG2* expression in a additional cohort of 63 HNSCC tumors and 30 normal mucosa (D).** Expression of *HES1*, *HEY1*, *JAG1*, and *JAG2* were significantly higher in HNSCC tumor tissues in comparison to normal tissues. Experiments were performed by Taqman realtime RT-PCR in triplicate and the data were normalized to *ACTIN* or *GAPDH* per sample.

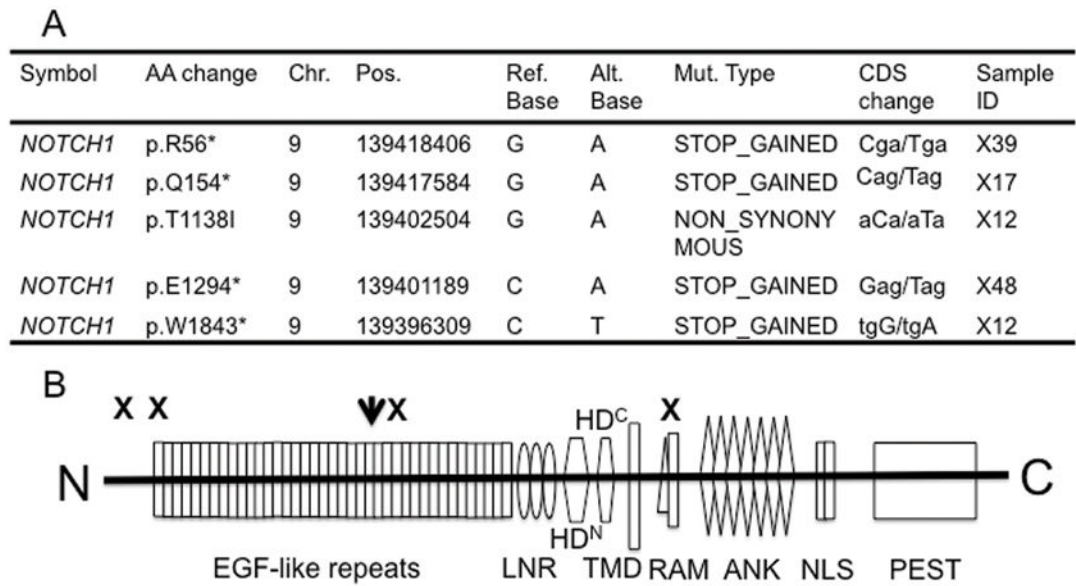


**Figure 5. *NOTCH1* mutations identified in the 37 HNSCC tumor tissues from the initial cohort of 44 HNSCC tumors and 25 normal mucosa**

**A.** *NOTCH1* mutations in the 37 HNSCC tumor tissues identified by whole exome sequencing. **B. Schematic depiction of mutations in *NOTCH1*.** EGF, epidermal growth factor; LNR, Lin12-*NOTCH* repeats; HD<sup>N</sup>, N-terminal heterodimerization domain; HD<sup>C</sup>, C-terminal heterodimerization domain; TMD, transmembrane domain; RAM, recombination signal-binding protein 1 for J- $\kappa$  (RBPj $\kappa$ ) association module; NLS, nuclear localization signal; PEST, proline, glutamic acid, serine/threonine-rich motifs. Black arrow (missense mutation) and "X" (truncating mutation) depict mutations observed in 4 out of the 37 HNSCC tumors observed in this study by targeted exome sequencing.

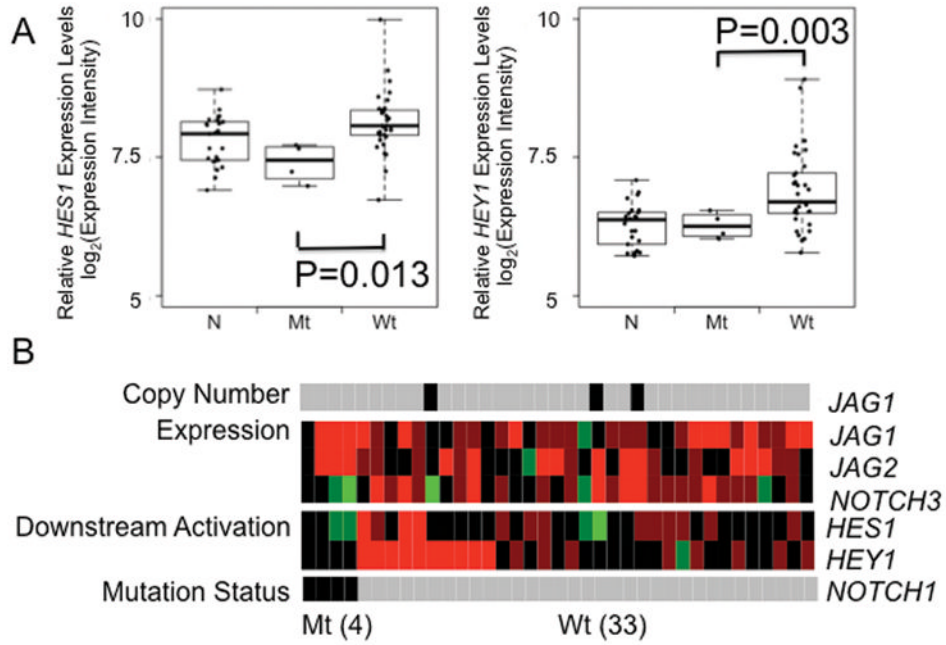


**Figure 6. A subset of wildtype *NOTCH1* HNSCC tumors has increased *HES1/HEY1* expression**  
**A. Comparison of *HES1/HEY1* expression among normal mucosa, *NOTCH1* mutant and wild type HNSCC tumors.** *NOTCH1* mutant HNSCC tumors had decreased *HES1/HEY1* expression in comparison to those in *NOTCH1* wildtype HNSCC tumors, and were similar to those in normal mucosa. N, normal mucosa, Mt, *NOTCH1* mutant HNSCC tumors, Wt, *NOTCH1* wild type HNSCC tumors. Boxes represent the interquartile range (25<sup>th</sup>–75<sup>th</sup> percentile) and horizontal lines inside the boxes indicate median. Whiskers indicate the minimum and maximum values. P value was calculated by using t test. **B. Heat-map display of copy number alteration (*JAG1*), transcriptional alteration (*JAG1*, *JAG2* and *NOTCH3*) and downstream activations (*HES1* and *HEY1*) of *NOTCH* pathway in 4 *NOTCH1* mutant and 33 *NOTCH1* wild type HNSCC tumors as defined in Figure 5.** Gray denotes HNSCC tumor with wild type *NOTCH1*, black, HNSCC tumor with mutant type *NOTCH1*. Red and green indicate over- or under-expression, respectively.

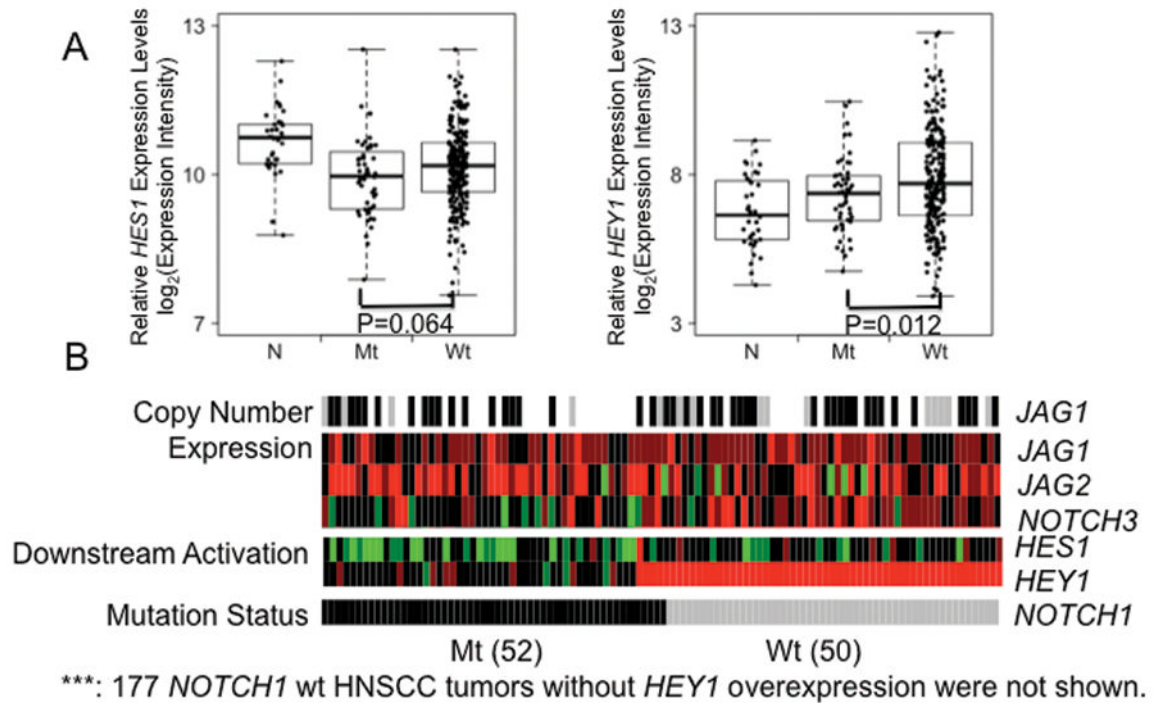


**Figure 7. Validation of the subset of wildtype *NOTCH1* HNSCC tumors with increased *HES1/HEY1* expression in TCGA HNSCC cohort of 279 tumor tissues and 37 adjacent normal tissues**

**A. Comparison of *HES1/HEY1* expression among adjacent normal mucosa, *NOTCH1* mutant and wild type HNSCC tumors.** *NOTCH1* mutant HNSCC tumors have decreased *HES1/HEY1* expression in comparison to those in *NOTCH1* wildtype HNSCC tumors. N, adjacent normal mucosa, Mt, *NOTCH1* mutant HNSCC tumors, Wt, *NOTCH1* wild type HNSCC tumors. Boxes represent the interquartile range (25<sup>th</sup>–75<sup>th</sup> percentile) and horizontal lines inside the boxes indicate median. Whiskers indicate the minimum and maximum values. P value was calculated by using t test. **B. Heat-map display of copy number alteration (*JAG1*), transcriptional alteration (*JAG1*, *JAG2* and *NOTCH3*) and downstream activations (*HES1* and *HEY1*) of *NOTCH* pathway in 52 *NOTCH1* mutant and 50 *NOTCH1* wild type HNSCC tumors (with *HEY1* overexpression) from the TCGA HNSCC cohort.** Gray denotes HNSCC tumor with wild type *NOTCH1*, black, HNSCC tumor with mutant type *NOTCH1*. Red and green indicate over- or under-expression, respectively.